

Gravitational Wave Phase shifts of black hole mergers in AGN Disks

HIROMICHI TAGAWA,¹ CONNAR ROWAN,² JÁNOS TAKÁTSY,³ LORENZ ZWICK,^{2,4} KAI HENDRIKS,^{2,4} WEN-BIAO HAN,^{1,5,6,7,8}
AND JOHAN SAMSING^{2,4}

¹*Shanghai Astronomical Observatory, Shanghai, 200030, People's Republic of China*

²*Niels Bohr International Academy, The Niels Bohr Institute, Blegdamsvej 17, DK-2100, Copenhagen, Denmark*

³*Institut für Physik und Astronomie, Universität Potsdam, Haus 28, Karl-Liebknecht-Str. 24-25, Potsdam, Germany*

⁴*Center of Gravity, Niels Bohr Institute, Blegdamsvej 17, 2100 Copenhagen, Denmark*

⁵*Hangzhou Institute for Advanced Study, University of Chinese Academy of Sciences, Hangzhou 310124, People's Republic of China*

⁶*School of Astronomy and Space Science, University of Chinese Academy of Sciences, Beijing 100049, People's Republic of China*

⁷*Taiji Laboratory for Gravitational Wave Universe (Beijing/Hangzhou), University of Chinese Academy of Sciences, Beijing 100049, People's Republic of China*

⁸*Key Laboratory of Radio Astronomy and Technology, Chinese Academy of Sciences, A20 Datun Road, Chaoyang District, Beijing 100101, People's Republic of China*

ABSTRACT

Ground-based gravitational wave (GW) detectors have discovered about 200 compact object mergers. The astrophysical origins of these events are highly debated, and it is possible that at least a fraction of them originate from dynamical environments. Among these, the disks of active galactic nuclei (AGN) are particularly interesting as promising environments, as some observed properties may be more readily produced there. When compact objects merge in these environments, acceleration from the central supermassive black hole (SMBH) or nearby companions is inevitable. Such acceleration induces a phase shift in the observed GW waveforms, which can serve as a useful tool to distinguish the underlying merging environments for each GW event. In this paper, we investigate the expected distribution of such acceleration-induced GW phase shifts, using a semi-analytical model combined with a one-dimensional AGN population synthesis code. We find significant contributions from three-body interactions involving a nearby third object. Our results indicate that the GW phase shift is likely to be larger compared to other channels, making it distinguishable by future GW facilities such as TianQin, DECIGO, Taiji, Einstein Telescope, and Cosmic Explorer. Interestingly, a notable fraction of mergers in fact exhibit a significant GW phase shift ($\gtrsim 1$ rad) at frequencies above 10 Hz, which could even be detectable by current GW detectors such as LIGO/Virgo/KAGRA. Additionally, if gas-hardening during three-body interactions is taken into account, the GW frequency can be boosted to $\gtrsim 10$ Hz, potentially further aiding in the detection of the phase shift.

Keywords: transients – stars: black holes –galaxies: active

1. INTRODUCTION

Gravitational waves (GWs) from about 200 binary black hole (BBH) mergers (The LIGO Scientific Collaboration et al. 2025a,b) have been discovered by LIGO/Virgo/Kagra (LVK) (LIGO Scientific Collaboration et al. 2015; Acernese et al. 2015; Akutsu et al. 2021); however, the underlying formation channels still remain highly debated. Promising channels include isolated binary evolution (e.g. Dominik et al. 2012; Kinugawa et al. 2014; Belczynski et al. 2016; Spera et al. 2019; Tanikawa et al. 2022), evolution of triple- or quadruple systems (e.g. Silsbee & Tremaine 2017; Antonini

et al. 2017a; Liu & Lai 2018; Fragione & Kocsis 2019), dynamical evolution in clusters (e.g. Banerjee 2017; Kumamoto et al. 2018; Rastello et al. 2018; Portegies Zwart & McMillan 2000; Samsing et al. 2014; O’Leary et al. 2016; Rodriguez et al. 2016), and active phases of galactic nucleus (AGN) disks (e.g. Bartos et al. 2017; Stone et al. 2017; McKernan et al. 2018; Tagawa et al. 2020b; Rowan et al. 2024b; Delfavero et al. 2025; Xue et al. 2025).

One of the key observables for distinguishing such formation channels apart is the orbital eccentricity when the GW source either forms or enters the LVK sensitivity band. Generally, a non-zero eccentricity indicates a dynamical origin, as something must have perturbed the BBH in question that brought it to merger. Such eccentric GW sources are expected to form in a wealth of

different dynamical environments (e.g. Samsing 2018a; Samsing et al. 2018; Samsing & D’Orazio 2018; Samsing et al. 2020a; Antonini et al. 2018; Rodriguez & Antonini 2018; Kremer et al. 2020; Zevin et al. 2021; Tagawa et al. 2021a), and is therefore an important probe of such systems. Interestingly, some observed GW sources already hint for a non-zero eccentricity in their GW form (e.g. Romero-Shaw et al. 2022; Gupte et al. 2024; Morras et al. 2025; de Lluç Planas et al. 2025). A particular interesting event is GW190521, believed to be associated with either strong precession or high eccentricity (Romero-Shaw et al. 2020; Gayathri et al. 2020; Gamba et al. 2023; Romero-Shaw et al. 2023, 2025), as well as possessing a relatively large mass (Abbott et al. 2020), beyond what is expected from pair-instability supernovae (Chatzopoulos & Wheeler 2012).

Many dynamical channels will, however, give rise to overlapping eccentricity-, mass- and spin distributions, and additional measures are therefore needed for disentangling the populations apart. One idea is to look for perturbations in the GW form, often referred to as GW phase-shift or GW de-phasing, caused by the nearby environment (e.g. Samsing et al. 2025; Hendriks et al. 2024a; Zwick et al. 2025b, 2024). For example, acceleration from a nearby third BH will result in a well-defined GW phase-shift (Meiron et al. 2017; Inayoshi et al. 2017; Wong et al. 2019; Yang et al. 2025; Hendriks et al. 2024b; Zwick et al. 2025c), whereas a gaseous background will cause GW phase shifts through additional energy and momentum-losses during inspiral (Chen et al. 2025a). In fact, there already exists hints for an accelerated GW source, GW190814 (Yang et al. 2025), which could indicate a merger near a massive object.

The formation of BBH mergers in so-called AGN disks around SMBHs have recently gained significant attention, as the gas component is a very effective catalyst for capturing the BHs into the disk, even if they did not originally form there, and bringing them together through migration (Bellovary et al. 2016; McKernan et al. 2018; Tagawa et al. 2020b; Grishin et al. 2024). While such AGN disk models do suggest various unique mass-, spin-, and eccentricity distributions (Gayathri et al. 2021; Yang et al. 2019a,b; Tagawa et al. 2020a, 2021a,b; Vaccaro et al. 2024; Xue et al. 2025; Li et al. 2025), similar mergers might form in other environments; however, it remains unexplored if state-of-the-art models for AGN disk mediated mergers also imply GW mergers with notable GW phase shift, which greatly could help identify their origin using present and future GW observatories.

With this motivation, we here explore the GW phase shift distribution of BBH mergers forming in AGN disks. For such mergers, there are at least two sources that can create a notable GW phase shift through acceleration. The first source is the acceleration from the central SMBH, which all the merging BBHs in the AGN disk experience. The second source of acceleration comes from

a possible nearby third object if the BBH was driven to merger through a chaotic interaction with an incoming single BH (Samsing et al. 2014), often referred to as a binary-single interaction. Such chaotic binary-single mergers can occasionally result in exceptionally large phase shifts due to the finite probability that the third object is very close to the BBH when merging (e.g. Hendriks et al. 2024b; Samsing et al. 2025). If one takes into account the surrounding gas from the AGN disk, the characteristic distance between the three objects can greatly decrease during the interaction, resulting in a further significant boost of the GW phase shift (e.g. Rowan et al. 2025b). Not only are such high acceleration events expected, but high eccentricity is also anticipated for a significant fraction of AGN mediated mergers (Samsing et al. 2022; Fabj & Samsing 2024; Fabj et al. 2025). Thus, GW phase shift and eccentricity can together provide valuable information for identifying BBH mergers in AGN environments. In addition, modulation is also expected in the GW signal, depending on the type of force and orbital configurations (e.g. Samsing et al. 2025; Zwick et al. 2024), which provide possibilities for breaking the mass-distance degeneracy in the acceleration.

The paper is organized as follow. In Sec. 2 we describe our model for how BHs form and interact in AGN disks, as well as the theory behind GW phase shifts caused by acceleration of nearby objects. Results are presented in Sec. 3, after which we conclude our study in Sec.4.

2. METHODS

2.1. Overview of models

We first provide an overview of the processes involved in the evolution and mergers of BHs in an AGN disk. We utilize the models from Tagawa et al. (2021b), where we track N -body particles in a 1D-setup that represent BHs as described below. The BHs are initially part of a nuclear star cluster surrounding the central SMBH, after which they are gradually captured by the AGN disk through accretion torques and gas dynamical friction (Syer et al. 1991; Generozov & Perets 2022; Wang et al. 2024; Rowan et al. 2025a; Whitehead et al. 2025a). BHs can also form in the outer regions of the AGN disk, where the gas is gravitationally unstable (Goodman 2003; Thompson et al. 2005; Stone et al. 2017; Chen et al. 2023; Epstein-Martin et al. 2025). Once embedded in the AGN disk, BHs migrate toward the SMBH due to type I/II torques from the disk (Duffell et al. 2014; Kanagawa et al. 2015, 2018). Because migration depends on BH mass, BHs of different masses will encounter each other in the disk, which can lead to binary formation primarily due to gas dynamical friction during two-body encounters (Goldreich et al. 2002; DeLaurentiis et al. 2023; Rozner et al. 2023; Li et al. 2023; Rowan et al. 2023, 2024a; Whitehead et al. 2024, 2025b; Qian et al. 2024; Dodici & Tremaine 2024) and partially through dynamical interactions during three-body en-

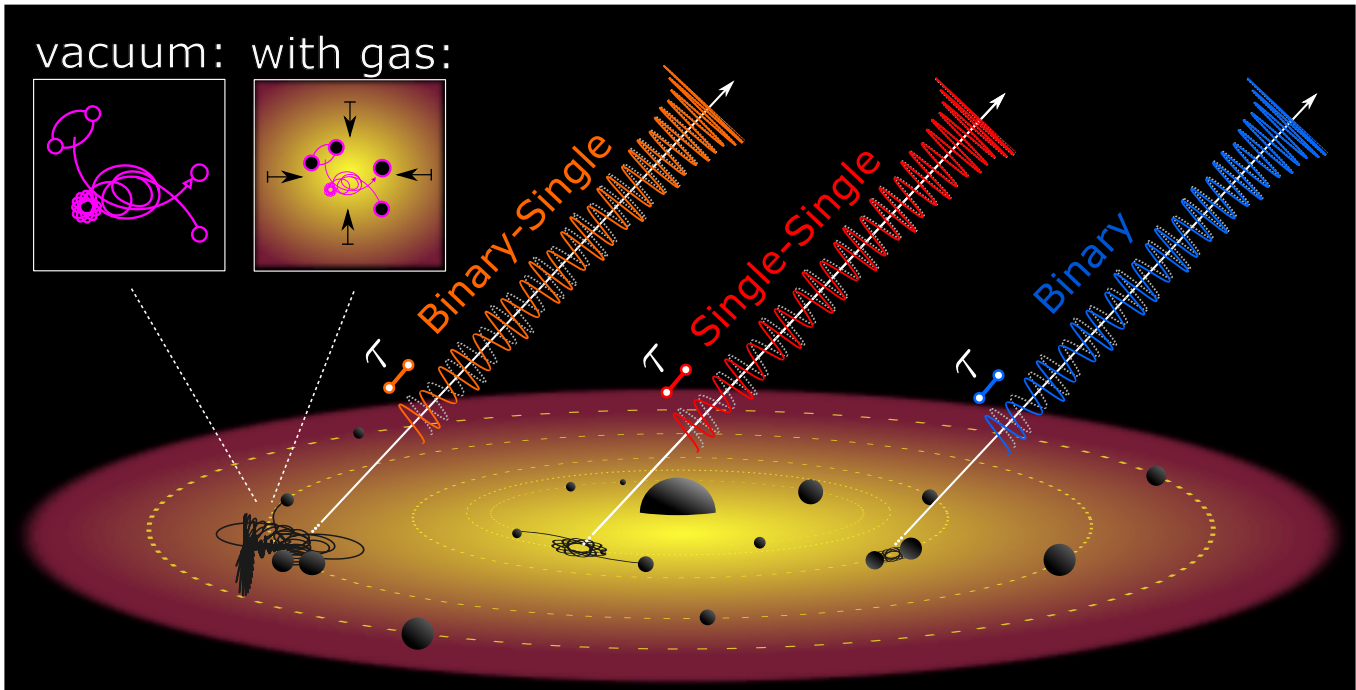


Figure 1. A schematic picture of BH mergers within an AGN disk and their GW phase shifts caused by acceleration from nearby compact objects. Non-GWC binaries and GWC binaries formed through single-single interactions experience strong gravitational acceleration due to the central SMBH. A GWC binary formed during binary-single interactions undergoes gravitational acceleration from its triple companion. In this case, gas drag may significantly harden the triple system, thereby boosting the GW frequency.

counters (Tagawa et al. 2020b). After formation, the semi-major axes (SMA) of these binaries generally decrease in the early phases due to gas dynamical friction (Li & Lai 2022, 2024; Dempsey et al. 2022; Dittmann et al. 2024, 2025). We also account for subsequent interactions with single stars, other BHs, and other BH binaries. For such few-body scatterings, we model the resultant changes in the binary SMA, velocities, orbital angular momentum directions, and eccentricities using the prescriptions outlined in Leigh et al. (2018) (see also Trani et al. 2024). In the final stage of BBH evolution, the separation and eccentricity evolve due to GW emission, with the merger assumed to occur when the pericenter distance becomes smaller than the innermost stable orbit. After the merger, the remnant BH receives a GW recoil kick following Lousto et al. (2012). We note that the BH dynamics we track in the AGN disk naturally produce a population of highly eccentric BH binaries, generated through the GWC mechanism in single-single encounters (e.g., O’Leary et al. 2009; Samsing et al. 2020a), and through binary-single interactions (Samsing et al. 2014, 2018; Tagawa et al. 2021a; Samsing et al. 2022). Lastly, BHs grow in mass through mergers and Eddington-limited accretion.

Using this framework, we investigate the evolution of BHs in models **M1**, **M2**, **M4**, and **M12**, as described in Tagawa et al. (2021a), although we do not include neutron stars. In short, **M1** is our fiducial model, as

detailed in Tagawa et al. (2021b). Table 1 lists its initial conditions. In model **M2**, binary-single interactions are constrained to a two-dimensional (2D) disk-like geometry instead of the 3D geometry used in **M1**. In model **M4**, the initial number of BHs is reduced by a factor of 10/3, and their initial velocity dispersion is increased by a factor of 5 relative to the fiducial model **M1**, which assumes a net orbital rotation of the massive objects considering vector resonant relaxation (Szolgyen & Kocsis 2018). In model **M12**, BHs do not migrate within the AGN disk. We consider these models because the evolution and mergers of BHs in AGN disks are primarily influenced by the differences they encompass. Compared to the results in Tagawa et al. (2021a), we adjusted the inner radius within which BHs are removed from 10^{-4} pc to 10^{-6} pc to ensure that we do not miss mergers occurring near the SMBH.

Below we outline the theory and calculation of the GW phase shift for the BBH mergers identified in our simulations.

2.2. Gravitational Wave Phase Shifts

When a BBH moves along an accelerated path, its position will deviate from its unperturbed linear motion by $l = (1/2)at^2$, where a is the acceleration, and t is the time until merger at $t = 0$ (Hendriks et al. 2024b; Samsing et al. 2025). This displacement along the line-of-sight relative to the observer equates to a delay in

Table 1. Model parameters for our fiducial values of model **M1**. In model **M2**, BH interactions occur in a 2D geometry. In model **M4**, the initial BH number is reduced to $N_{\text{BH,ini}} = 6000$ and the initial velocity anisotropy parameter is enhanced to $\beta_v = 1$. In model **M12**, migration is not taken into account.

Parameter	Fiducial value
Spacial directions in which BS interactions occur	isotropic in 3D
Mass of the central SMBH	$M_{\text{SMBH}} = 4 \times 10^6 M_{\odot}$
Gas accretion rate at the outer radius of the simulation (5 pc)	$\dot{M}_{\text{out}} = 0.1 \dot{M}_{\text{Edd}}$ with $\eta = 0.1$
Fraction of pre-existing binaries	$f_{\text{pre}} = 0.15$
Power-law exponent for the initial density profile for BHs and NSs	$\gamma_{\rho, \text{BH}} = 0$
Initial velocity anisotropy parameter such that $\beta_{v, \text{BH}} v_{\text{kep}}(r)$ is the BH velocity dispersion	$\beta_{v, \text{BH}} = 0.2$
Efficiency of angular momentum transport in the α -disk	$\alpha_{\text{SS}} = 0.1$
Stellar mass within 3 pc	$M_{\text{star, 3pc}} = 10^7 M_{\odot}$
Stellar initial mass function slope	$\delta_{\text{IMF}} = 2.35$
Angular momentum transfer parameter in the outer star forming regions (Eq. C8 in Thompson et al. 2005)	$m_{\text{AM}} = 0.15$
Accretion rate in Eddington units onto stellar-mass COs with a radiative efficiency $\eta = 0.1$	$\Gamma_{\text{Edd, cir}} = 1$
Numerical time-step parameter	$\eta_t = 0.1$
Number of radial cells storing physical quantities	$N_{\text{cell}} = 120$
Maximum and minimum r for the initial CO distribution	$r_{\text{in, BH}} = 10^{-6}$ pc, $r_{\text{out, BH}} = 3$ pc
Initial number of BHs and NSs within 3 pc	$N_{\text{BH, ini}} = 2 \times 10^4$

the GW arrival time given by $\tau = l/c$, where c is the speed of light. In our case, where a BBH is accelerated by a nearby third object BH of mass m_3 , the maximum displacement in time is

$$\tau(t) = \frac{l}{c} = \frac{1}{2} \frac{G m_3}{c} \frac{t^2}{R^2} \quad (1)$$

where G is the gravitational constant, and R is the distance to the third body from the BBH's center-of-mass (COM). This displacement in arrival time, often referred to as the Romer-Delay, can be translated into a GW phase shift. We define this phase shift as the observed angular displacement in units of radians between the reference and the accelerated binary, approximately given by

$$\begin{aligned} \Delta\phi(t) &\approx 2\pi\tau(t)/T(t), \\ &\approx \frac{1}{2} \frac{G^{3/2}}{c} \frac{m_3 m_{12}^{1/2}}{R^2} \times \frac{t^2}{a(t)^{3/2}} \end{aligned} \quad (2)$$

where we have used Eq. (1), $m_{12} = m_1 + m_2$ is the total mass of the BBH, and that the (inner) orbital period of the BBH at time t can be estimated as,

$$T(t) = 2\pi\sqrt{a(t)^3/Gm_{12}}. \quad (3)$$

Using the relations from Peters (1964), $\Delta\phi(t)$ from Eq. (2) can be expressed in the circular limit ($e = 0$)

as a function of time as,

$$\Delta\phi(t) \approx \frac{c^{7/8} G^{3/8}}{2} \left(\frac{5}{256}\right)^{3/8} \times \frac{m_3}{R^2} \frac{m_{12}^{1/8}}{m_1^{3/8} m_2^{3/8}} \times t^{13/8}. \quad (4)$$

This relation can be further expressed in terms of the evolving GW frequency, which in the circular limit equals $f = 2/T$, leading to

$$\Delta\phi(f, e = 0) \approx \frac{c^9 G^{-7/3}}{2\pi^{13/3}} \left(\frac{5}{256}\right)^2 \times \frac{m_3}{R^2} \frac{m_{12}^{2/3}}{m_1^2 m_2^2} \times f^{-13/3}. \quad (5)$$

These equations are valid only for circular binaries; however, BBHs formed dynamically often retain eccentricities when observed. One way of defining the GW phase shift in the eccentric limit is to keep the definition from Eq. (2), with the addition that the evolution of the SMA a then also depends on the time-evolving eccentricity. Using the relation $a(e)$ from Peters (1964) in the high eccentricity limit,

$$a(e) \approx \frac{2r_0 e^{12/19}}{(1-e^2)} \frac{g(e)}{g(1)}, \quad (e_0 \approx 1). \quad (6)$$

where

$$g(e) = (1 + 121e^2/304)^{870/2299}, \quad (7)$$

and $r_0 = a_0(1 - e_0)$, we can write Eq. (2) as,

$$\begin{aligned} \Delta\phi(e) &\approx \frac{288\sqrt{2}}{85^2 g(1)^{13/2}} \frac{c^9}{G^{9/2}} \times \frac{m_3}{R^2} \frac{r_0^{13/2}}{m_1^2 m_2^2 m_{12}^{3/2}} \\ &\times e^{78/19} (1 - e^2)^{1/2} g(e)^{13/2} \\ &\approx \frac{288\sqrt{2}\pi^{-13/3}}{85^2 g(1)^{13/2}} \frac{c^9}{G^{7/3}} \times \frac{m_3}{R^2} \frac{m_{12}^{2/3}}{m_1^2 m_2^2} \times f_0^{-13/3} \\ &\times e^{78/19} (1 - e^2)^{1/2} g(e)^{13/2}, \end{aligned} \quad (8)$$

where f_0 is the GW peak frequency, f , and

$$f(a, e) \approx \frac{1}{\pi} \sqrt{\frac{Gm_{12}}{r(a, e)^3}}, \quad (9)$$

is evaluated at the initial values for a , e , i.e. $f_0 = f(a_0, e_0)$. As seen in Eq. (8), the dependence on e factors out into the function $F(e) = e^{78/19} (1 - e^2)^{1/2} g(e)^{13/2}$, with a maximum given by $e_m \approx 0.95$. Using the approximate relation for the GW peak frequency given by Eq. (9), Eq. (8) can be approximated as (Samsing et al. 2025),

$$\Delta\phi(f) \approx \Delta\phi(f, e = 0) \times (1 + (f_0/f))^7 (1 - (f_0/f))^{1/2}. \quad (10)$$

Note here that when $f \gg f_0$ it transitions correctly into the circular case.

Finally, we note that our general definition of the GW phase shift from Eq. (2) is natural and correct when the binary is circular, as it essentially provides a measure for how well we can localize a possible displacement τ relative to the period T . However, when the binary is eccentric, the period over which most of the GW signal is emitted is much shorter than the orbital time, allowing for a much better resolution for measuring a possible displacement, τ (e.g. Zwick et al. 2025a,e; Takátsy et al. 2025; Zwick et al. 2025d). If we denote the GW burst-width in the high eccentricity limit by dt , it follows that

$$dt \approx \frac{1}{f} \quad (11)$$

where f refers to the GW peak frequency from Eq. (9). Using this instead of T in Eq. (2), it follows that

$$\begin{aligned} \Delta\phi_p &\approx 2\pi\tau(t)/dt, \\ &\approx (n_p/2) \times \Delta\phi \end{aligned} \quad (12)$$

where $n_p \geq 2$ is the n 'th-harmonic corresponding to the GW peak frequency harmonic, and $\Delta\phi$ is the GW phase shift defined in Eq. (2). The value for n_p will be $\simeq 2(1 + e)^{1.1954} / (1 - e^2)^{3/2} \gg 2$ in the high eccentricity limit (Wen 2003; Hamers 2021), indicating that the GW phase shift can therefore be significantly larger than the one directly carried over from the circular limit. In this study, we primarily consider results from the conservative estimate based on the fundamental harmonic with

the GW phase shift given by Eq. (2), but we will also show a few cases where the definition from Eq. (12) is used. As waveforms required for a full signal-to-noise (S/N) analysis are not yet available, we reserve any S/N calculations for upcoming studies.

2.3. AGN Binary Black Hole Merger Types

BBHs merging through different dynamical path ways will be considered differently in our analysis, as they give rise to different outcomes and observables. In the following, we outline and define the three main merger channels arising from our AGN disk models.

(1) Binary Merger (non-GWC): This type of merger happens between two BHs that evolve in the AGN disk while not being bound to anything else than each other and the central SMBH. Such BBHs are often driven together through a combination of gas-drag and GW emission (Bartos et al. 2017; Tagawa et al. 2020b). They might have undergone previous interactions with other objects while migrating through the disk, but none of these objects are near at merger, which further implies that they generally merge on near circular orbits. For calculating the associated GW phase shift, we use the equations from Sec. 2.2 with m_3 and R set to the mass of the SMBH and the distance from the BBH COM to the SMBH, respectively. The orbital elements a and e for each BBH merger is taken directly from the output of our AGN model. Throughout the paper we refer to these mergers as ‘non-GWC’.

(2) Single-Single Merger (GWC-SS): These mergers are formed through a GW single-single capture between two initially unbound BHs. In our models, this process is often taking place in the inner parts of the AGN disk. For calculating the GW phase shift of these mergers we follow the same procedure as for the ‘non-GWC’ mergers above. Throughout the paper we refer to these as ‘GWC-SS’.

(3) Binary-Single Merger (GWC-BS): These mergers occur during a binary-single interaction, while the third object is still bound to the merging BBH (see Samsing et al. 2014; Samsing & Ramirez-Ruiz 2017; Samsing 2018b). This type of merger is particularly interesting, as the third object often is so close that the resultant acceleration on the BBH COM dominates over the acceleration from the SMBH. These types of mergers can therefore result in relatively high GW phase shifts. In addition, if one takes into account that the surrounding gas can harden the system while the three BHs are interacting (Rowan et al. 2025b), the GW phase shift can get even larger. We explore both cases in the following. Without gas effects we calculate the GW phase shift by setting m_3 equal to the third bound BH, and R equal to the initial SMA of the BBH before the interaction as this sets the characteristic length scale of the system. When gas is included, we scale down the scales of the entire system by a fraction inspired from full hydro-simulations of triple scatterings in an AGN disk

(Rowan et al. 2025b). We acknowledge these prescriptions are only approximate, but it is beyond this work to perform a full PN/gas few-body scattering exploration for all interactions that might take place in our AGN disk models (see Tagawa et al. 2021b). Throughout the paper we refer to these mergers as ‘GWC-BS’.

The majority of merging binaries ($\sim 90\%$) were initially formed through the gas-capture mechanism (Tagawa et al. 2020b), where a fraction of the energy of the encounter is dissipated via the gas (see Rowan et al. 2023, 2024a; Whitehead et al. 2024, 2025b). The gas-capture model in our four models was compared with that derived from hydrodynamical simulations in Rowan et al. (2024b), showing good agreement.

3. RESULTS

In the following sections, we present the distribution of the phase shift expected in the AGN channel, and discuss the effects of gas and eccentricity on the phase shift.

3.1. Distribution of Gravitational Wave Phase Shifts

Results for our fiducial **M1** model are presented in Fig. 2, which shows the evolution of the eccentricity (top) and the GW phase shift (bottom), respectively, as a function of the peak GW frequency, for our considered merger types. As seen in the figure, binary mergers (non-GWC) primarily form at low GW peak frequencies of $\lesssim 0.01\text{--}0.1$ Hz, with an eccentricity distribution shaped by a combination of previous scatterings and the mechanisms behind the binary assembly. This population does exhibit a significant GW phase shift caused by the acceleration of the central SMBH, but only at lower frequencies as it rapidly decreases $\propto f^{-13/3}$ (Zwick et al. 2025c). This type of GW phase shift has been studied in the literature before (Vijaykumar et al. 2023), and a recent study even presents tentative evidence of acceleration in a similar configuration (Yang et al. 2025). The majority of the non-GWC population will be a prime observational target for upcoming deci-Hertz detectors such as DECIGO (Yagi & Seto 2011), DO (Arca Sedda et al. 2020), and ALIA (Mueller et al. 2019). Distributions of the cumulative phase shifts above 10 Hz and 0.1 Hz are presented in Figs. 3 and 4, respectively.

GWC-BS mergers primarily form with an initial peak GW frequency of $\gtrsim 1$ Hz, as the third bound object imposes natural limits on the initial SMA and eccentricity of the merging BBH (Samsing et al. 2014). This influence of the third object also leads to GW phase shifts that are significantly higher than those arising from a distant SMBH. The GWC mergers therefore constitute a distinct population, that we observe in our AGN disk models, typically exhibiting phase shifts of $\gtrsim 0.1$ rad near the LVK band and even beyond. GWC-SS mergers form differently, and their acceleration are entirely due to the SMBH and how close the disk model allows them to form. Therefore, these mergers can occur at all

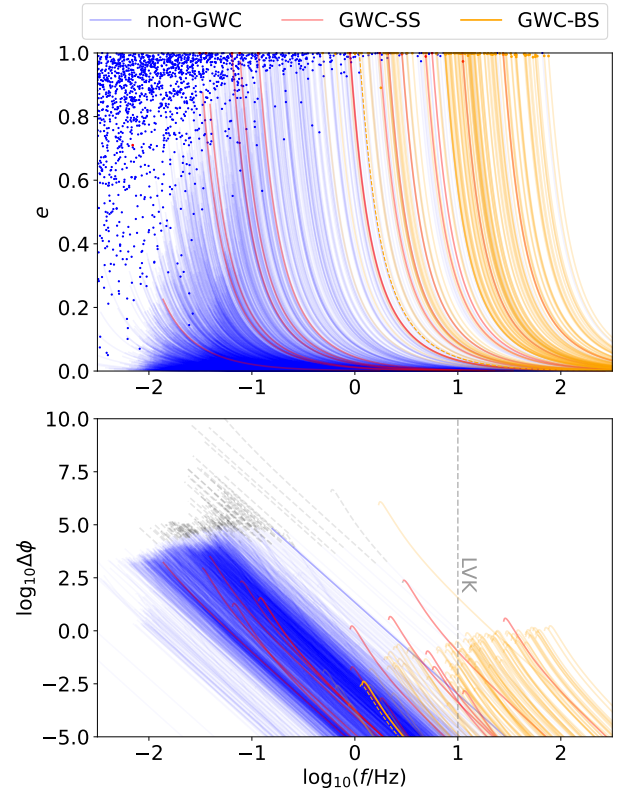


Figure 2. The evolution of the orbital eccentricity and the cumulative phase shift until mergers for model **M1**. Points represent values at binary formation, and lines represent their evolution. Blue, orange and brown, and red lines display the results for mergers due to non-GWC processes, mergers due to the GWC mechanism during binary-single interactions, and those during single-single interactions, respectively. For GWC binaries during binary-single interactions, the solid lines correspond to cases where the acceleration from the bound third BH is dominant, while the dashed lines correspond to cases where the acceleration from the SMBH is dominant. In the lower panel, the dashed gray lines depict the evolution for phases in which the binary moves more than 1/4 of the orbit around its companion (third BH or SMBH) before merging. The lines are shown for the final 5 yr to merger, and are not connected to the points in the upper panel for cases with long merger time. The gray vertical dashed line in the lower panel represents the typical value for the LVK sensitivity band.

frequencies with large phase shifts, as also seen in the figure. While the GWC-BS mergers can be studied with local scattering experiments, the evolution of GW-SS mergers and their phase shifts depend sensitively on all the binary evolution mechanisms through the disk and the global disk properties.

3.2. Distribution of Binary Accelerations

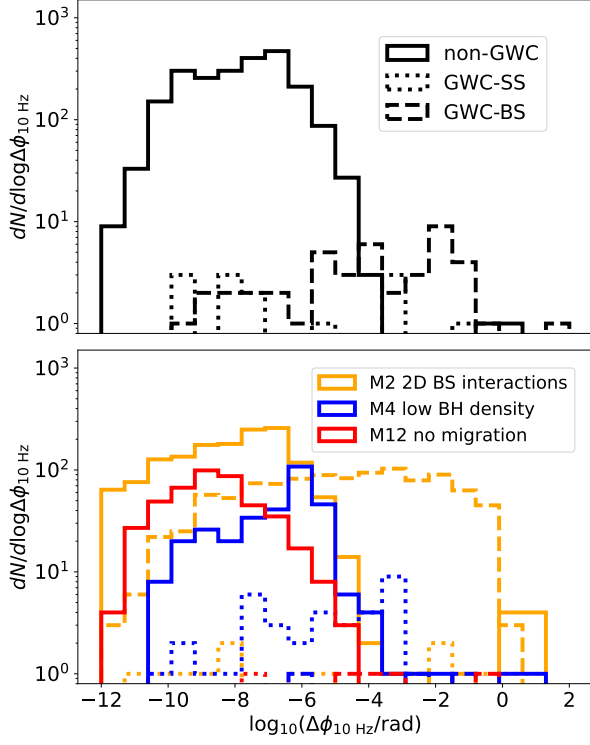


Figure 3. The distribution of cumulative phase shifts above 10 Hz. Solid, dashed, and dotted lines represent the results for mergers due to non-GWC processes, mergers due to the GWC mechanism during binary-single interactions, and those during single-single interactions, respectively. The upper panel shows the result for model **M1**, and orange, blue, and red lines in the lower panel shows those for models **M2**, **M4**, and **M12**, respectively.

Fig. 5 shows the distribution of the BBH COM acceleration for our considered merger types. The top plot shows results for the **M1**-model, where the bottom plot shows the total distribution across all three merger types for the remaining models, **M2**, **M4**, and **M12**. The solid- and dashed lines illustrate the acceleration on the BBH COM dominated by the SMBH and a nearby third-object, respectively. As seen, non-GWC mergers peak at around $\sim 1\text{ cm s}^{-2}$ and GWC mergers peak at much higher values. Notably, these accelerations are significantly larger than those typically expected for the triple channel (Antonini et al. 2017b, 2018). To distinguish the underlying environments, detecting these accelerations is crucial.

According to Zwick et al. (2025c), for BH masses ranging from 5 to 200 M_{\odot} and redshifts between 0 and 5, a significant fraction of mergers with accelerations of $a \sim 10^2\text{--}10^4\text{ cm s}^{-2}$, $a \gtrsim 10^6\text{ cm s}^{-2}$, and $a \gtrsim 10^7\text{ cm s}^{-2}$ are detectable by the Einstein Telescope and Cosmic Explorer, as well as during the *A#* and O4 sensitivity

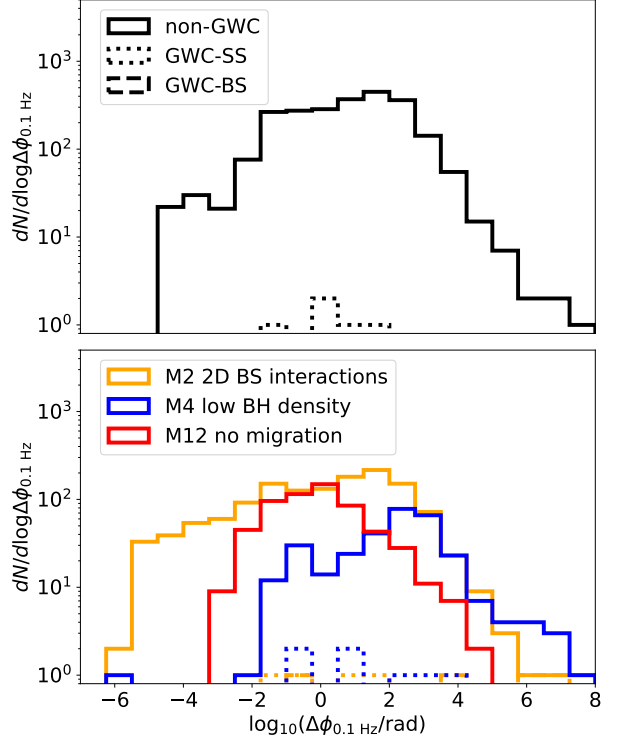


Figure 4. Same as in Fig. 3, but for cumulative phase shifts above 0.1 Hz.

observations of LIGO/Virgo/KAGRA, respectively. As seen in Fig. 5, a certain fraction of mergers meets these conditions and may therefore serve as promising signatures for mergers in AGN disks, potentially detectable even by the O4 sensitivity. These large accelerations are also consistent with the value ($\sim 0.0015\text{c s}^{-1}$) implied for GW190814 (Yang et al. 2025) shown in purple in Fig. 5, which could suggest a GWC-BS origin. If binary-single interactions occur in a two-dimensional geometry (model M2), a larger fraction of the GW mergers exhibit higher GW phase shifts, as seen in the lower panel of Fig. 3, due to the significantly higher occurrence rate of GWC-BS mergers (Samsing et al. 2020b). Additionally, the fraction of mergers with significant phase shifts ($\gtrsim 10^{-2}$ rad) is less affected by the number density of BHs, although the total number of mergers is influenced (blue lines). Similar to the fiducial model, binaries undergo multiple binary-single interactions before mergers, resulting in a comparable fraction of GWC mergers. The same reasoning applies to the model without migration (red lines). The fraction of mergers with a cumulative phase shift exceeding 0.1 rad above 10 Hz is 0.2%, 1%, 0.4%, and 0.3% for models **M1**, **M2**, **M4**, and **M12**, respectively, where the fractions exceeding 1 rad are 0.07%, 0.2%, 0.4%, and $< 0.2\%$.

Given a fixed SMBH mass, the amount of acceleration is determined by the distance to the SMBH, R , whose

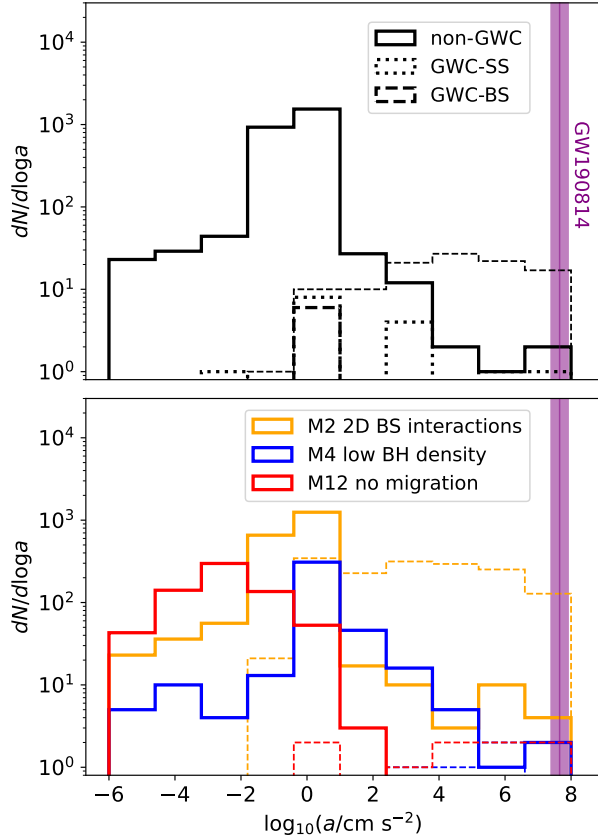


Figure 5. The distribution of acceleration from the third body at binary formation. In the upper panel, solid, dotted, and dashed lines represent the results for model **M1** for mergers occurring due to non-GWC processes, mergers resulting from the GWC mechanism during binary-single interactions, and those occurring during single-single interactions, respectively. In the lower panel, blue, orange, and red lines represent the results for all the mergers for models **M2**, **M4**, and **M12**, respectively. In upper and bottom panels, thick lines indicate cases where the acceleration from the SMBH is dominant, while thin dashed lines indicate cases where the acceleration from the third bound BH is dominant. The purple vertical box and line represent 90% confidence intervals and median for acceleration in GW190814 suggested by Yang et al. (2025).

distribution is represented by the solid lines in Fig. 6 for all four models. In the fiducial **M1**-model (black lines), distances are concentrated around ~ 0.01 pc, as migration slows down in these regions due to the formation of deep gaps (Tagawa et al. 2020b; Gilbaum et al. 2025). In the **M12**-model without migration (solid red lines in Fig. 6), mergers occur at ~ 0.1 pc, resulting in lower acceleration from the SMBH and smaller phase shifts

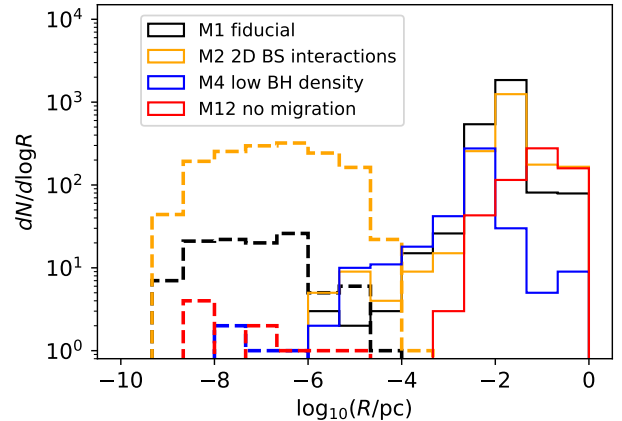


Figure 6. The distribution of the distance to the third body. Black, orange, blue, and red lines represent the results for models **M1**, **M2**, **M4**, and **M12** respectively. The thick lines represent the distance to the SMBH in cases where the acceleration from the SMBH is dominant, while dashed lines represent the distance to the third bound BH in cases where the acceleration from the BH is dominant.

(as shown by the solid red lines in the lower panels of Figs. 5 and 4).

Although we have not explicitly included migration traps or thermal torques in the fiducial model, we consider their potential effects. Incorporating migration traps into the fiducial model, following the methodology described by Bellovary et al. (2016), BH mergers do not occur at $R \leq 10^{-4}$ pc. Consequently, both non-GWC and GWC-SS mergers with $a \gtrsim 10^4$ cm s $^{-2}$ and $\Delta\Phi \gtrsim 10^{-3}$ rad at 10 Hz are suppressed. Conversely, by considering thermal torques in the prescriptions described by Jiménez & Masset (2017) and Grishin et al. (2024), BHs are driven toward $R \leq 10^{-4}$ pc likely due to gap formation and saturation effects. The resulting distributions for acceleration and phase shift are similar to those in the fiducial model. Since mergers occurring at $R \leq 10^{-4}$ pc are relatively minor, the influence of these prescriptions on the phase shift remains limited.

3.3. Gas effects

The effects of gas during binary-single interactions are not considered or included in any of the dynamical prescriptions used in the AGN models employed here (Tagawa et al. 2021a). This omission is largely justified if gas drag is described by the formulas for gas dynamical friction (Ostriker 1999), as this generally would lead to very small effects (Tagawa et al. 2020b) due to the

relatively high velocities close to merger. However, recently [Rowan et al. \(2025b\)](#) performed two-dimensional hydrodynamical simulations of binary-single scatterings in a disk-like environment and found that the entire triple system typically undergoes significant shrinkage due to interactions with the surrounding gas. Furthermore, since the kinetic energy of the interacting objects is generally rapidly dissipated, it was found that the interactions can involve many more close encounters compared to the vacuum case before terminating (see also [Wang et al. 2025a,b](#)). Shrinkage of the system is efficient only during interactions, presumably because small Bondi-Hoyle-Lyttleton radii enable gas dynamical friction from high-density gas nearby BHs. Specifically, [Rowan et al. \(2025b\)](#) showed that triple systems during the interaction can easily shrink by a factor of ~ 20 , with significant implications for the resultant phase shifts.

Here we construct a model for gas drag that better aligns with the simulation results. According to [Rowan et al. \(2025b\)](#), the captured gas accumulates around the binary system. Once binary-single interactions occur, this accumulated gas facilitates the binary evolution, by dissipating the kinetic energy of the third body. Assuming that a significant fraction of the captured gas is ejected at an orbital speed of the binary (v_{orb}) multiplied by a factor ($f_{\text{ej}} \sim \mathcal{O}(1)$), we tentatively prescribe the energy dissipation rate as

$$\frac{dE}{dt} \sim \frac{M_{\text{ret}} f_{\text{ej}}^2 v_{\text{orb}}^2}{t_{\text{decay}}}, \quad (13)$$

where M_{ret} is the retained gas mass, defined as the accumulated captured gas mass minus the depleted gas mass, and t_{decay} is the timescale of binary evolution during binary-single interactions, typically ~ 1 –100 times the dynamical time of the binary ([Samsing et al. 2014](#); [Rowan et al. 2025b](#)). The uncertainty in this timescale does not affect the results below. Using $v_{\text{orb}}^2 \sim G(m_1 + m_2)/R$ and $E = Gm_3(m_1 + m_2)/R$, Eq. (13) can be reformulated as

$$E \sim E_0 \exp\left(\frac{f_{\text{ej}}^2 M_{\text{ret}} t}{m_3 t_{\text{decay}}}\right), \quad (14)$$

which is valid for $t \leq t_{\text{decay}}$. Using the results from the simulations of [Rowan et al. \(2025b\)](#), and evaluating the gas capture rate with Eq. (1) of [Tagawa et al. \(2022\)](#) (which can predict capture rates, at least for two-dimensional simulations, [Whitehead et al. 2024](#)), we find $f_{\text{ej}} \sim 1.1$ (although the variability is high, see Fig. 8 of [Rowan et al. 2025b](#)). This suggests that the assumption that most captured gas is ejected at a velocity $\sim v_{\text{orb}}$ is consistent with the simulation. Note that in [Wang et al. \(2025b\)](#), gas disappears due to accretion and M_{ret} is somewhat uncertain, making this evaluation more challenging.

Since three-body systems shrink due to gas effects, we need to consider the resulting changes in the proper-

ties of GWC binaries at formation. When the distance to the third body is reduced by some factor, the pericenter distance within which GWC binaries form also changes. The maximum pericenter distance is proportional to the relative velocity as $r_{\text{p,max}} \propto v^{-4/7}$ (e.g. [O’Leary et al. 2009](#)). Assuming that the relative velocity is roughly given by the Keplerian velocity of the binary and that the Keplerian velocity scales as ($v \propto R^{-1/2}$), then the maximum pericenter distance then scales as $r_{\text{p,max}} \propto R^{2/7}$ ([Samsing et al. 2014](#); [Samsing 2018b](#); [Samsing & Hotokezaka 2021](#)). We assume that the initial semi-major axis of the binary is reduced by the same factor as the reduction in R caused by gas effects. The eccentricity at GWC binary formation is adjusted to ensure that the pericenter distance decreases by the same factor corresponding to the reduction of $r_{\text{p,max}}$. In this way, both the initial peak frequency of the binary and the cumulative phase shift are affected, reflecting the shrinkage of the three-body systems due to gas effects.

In realistic environments, we can expect the retained mass to saturate because of depletion through accretion and wind mass loss. In our simulation, assuming that the captured gas can be retained around the binary for the viscous timescale, we set $M_{\text{ret}} \sim \dot{M}_{\text{cap}} t_{\text{vis}}$, where \dot{M}_{cap} is the gas capture rate, and t_{vis} is the viscous timescale at the circularization radius for the captured gas. The circularization radius is set to $r_{\text{circ}} = f_{\text{circ}} r_{\text{Hill}}$, where r_{Hill} is the Hill radius, and f_{circ} is a factor representing the ratio between the circularization radius and the Hill radius ([Sagynbayeva et al. 2025](#)). Since the capture rate is highly super-Eddington, we assume the disk is thick, with $t_{\text{vis}} \sim t_{\text{orb}}(r_{\text{circ}})/\alpha_{\text{ss}}$, where $t_{\text{orb}}(r)$ is the orbital timescale at radius r from the binary center, and $\alpha_{\text{ss}} \sim 0.1$ is the alpha-viscosity parameter. By incorporating $t = t_{\text{decay}}$ and $f_{\text{ej}} = 1.1$ into Eq. (14), we can calculate the final energy of the three-body system.

Conversely, when $M_{\text{ret}} \gg m_3$, Eq. (14) overestimates the final energy because, before all the retained gas is ejected, the binary can merge via the GWC mechanism. [Rowan et al. \(2025b\)](#) estimated that during ~ 20 intermediate states in binary-single interactions, once the binary is hardened to $\lesssim 10^4$ Schwarzschild radii, $\gtrsim 80\%$ of binaries merge. Reflecting this, we assume that binaries are maximally hardened to $\sim 10^4$ times the Schwarzschild radius of the primary BH.

Fig. 7 compares the cumulative phase shifts without (upper panel) and with gas (lower panel). The distance to the third body is reduced by gas effects by a factor of $\gtrsim 1.1$ in $\sim 30\%$ of the GWC mergers during binary-single interactions (green lines). These are more frequent at lower-frequency bands, since binaries at higher frequencies often exceed the limit of $\sim 10^4$ times the Schwarzschild radius. When the distance to the third body is reduced by the gas effect, the GW frequency is shifted to higher values, while the cumulative phase shift is less affected. This is because the GW frequency scales

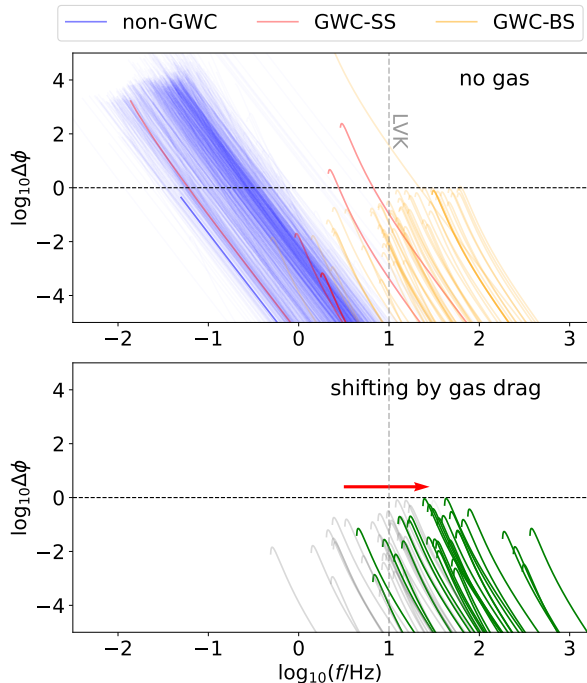


Figure 7. The upper panel is the same as the lower panel of Fig. 2. In the lower panel, the results for GWC-BS mergers are shown. The cases in which the distance to the third bound body is reduced by a factor of ≥ 1.1 due to gas effects are represented by green lines, while those without gas effects are shown with gray lines. Cases where the distance change is ≤ 1.1 are not displayed.

as $f_0 \propto r_0^{-3/2} \propto R^{-3/7}$, while the cumulative phase shift scales as $\propto f_0^{-13/3} R^{-2} \propto R^{-1/7}$ (Eq. 8). Thus, the dependence of the cumulative phase shift on R is weak (e.g. Samsing et al. 2025). As the GW frequency typically shifts above ~ 10 Hz, the phase shift may be more easily constrained by LIGO/Virgo/KAGRA, since it accumulates predominantly in frequency bands where these detectors are more sensitive. Importantly, these results suggest that a significant fraction of non-GWC mergers may also merge as GWC mergers due to the boosting of the peak frequency by gas effects. This would have a substantial impact on observables and is worth assessing in future studies.

Additionally, we have not included the effects of gas on the GWC mechanism during single-single encounters or for non-GWC mergers. In the former case, the effective masses of the binary components are enhanced by surrounding circum-BH disks (Rowan et al. 2024a), which increases the probability of the GWC mechanism, as the maximum pericenter distance within which GWC can occur is proportional to the total mass of the binary, assuming a fixed mass ratio (Quinlan & Shapiro 1989). Incorporating this effect could further boost the rates

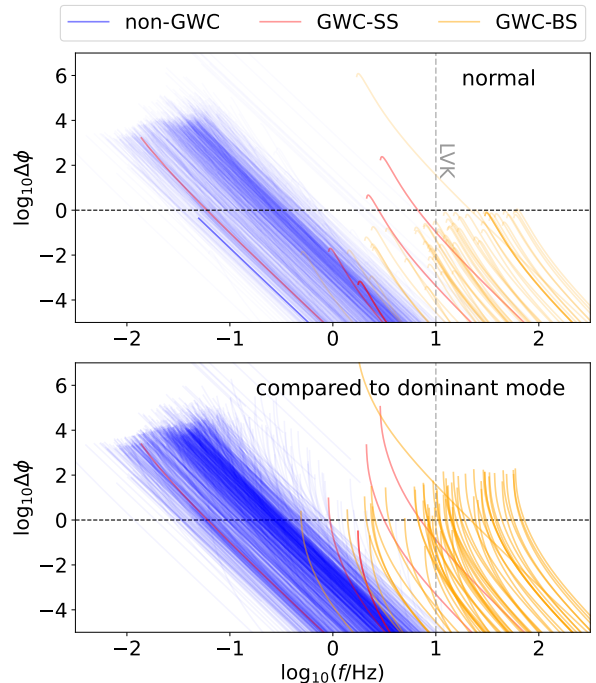


Figure 8. The upper panel is the same as the lower panel of Fig. 2. In the lower panel, we consider the phase shift relative to the period of the GW mode that predominantly contributes to the amplitude of the GW emission, as given by Eq. (12).

of mergers with high eccentricities and significant phase shifts.

Furthermore, gas can cause a phase shift through its torques. This effect would be more easily observable for non-GWC mergers, since the time from the last scattering to merger is longer. Such torques are expected to be detectable by LISA, TianQin, and Taiji (Dutta Roy et al. 2025; Chen et al. 2025b).

3.4. Eccentric Burst Sources

We have defined the phase shift as the change in the number of cycle counts of the GW signal, with the frequency given by the orbital frequency. This limit naturally bridges to the well studied circular case. However, when the binary becomes highly eccentric, higher modes dominate the GW signal, which in fact allows for a much better determination of the phase shift as also argued in Sec. 2.2 and recently in Zwick et al. (2025a,e,d) and Takátsy et al. (2025). To illustrate how the phase shift is enhanced by considering different modes, Fig. 8 presents the phase shift defined by the change in cycles calculated with the orbital frequency (upper panel) and that with the dominant GW frequency (lower panel).

For binaries formed via GWC (orange and red lines in Fig. 8), the high eccentricities cause the phase shift relative to cycles with the dominant mode frequency

to exceed ~ 1 rad after binary formation. Thus, the phase shift becomes significant depending on whether it is measured with respect to the orbital frequency or the dominant GW mode frequency. Assessing the detectability of these shifts in highly eccentric systems is a topic for future work.

4. CONCLUSIONS

In this study, we have predicted the distribution of phase shifts caused by acceleration from nearby objects for BH mergers in AGN disks. These predictions are based on a semi-analytical model combined with one-dimensional N -body simulations. Our key findings are as follows:

1. For all mergers, binaries experience strong acceleration from the central SMBH. Non-GWC binaries undergo moderate acceleration of $\sim \text{cm s}^{-2}$, which is detectable by future GW facilities such as the Einstein Telescope and Cosmic Explorer.
2. GWC binaries formed during binary-single interactions experience strong accelerations caused by a third body near the merging binaries, resulting in significant phase shifts. Additionally, GWC binaries formed during single-single interactions are located close to the SMBH. These binaries are subject to strong accelerations, which are larger than those expected in other formation channels. Furthermore, a small fraction (~ 0.1 – 1%) of merg-

ers exhibit a substantial cumulative phase shift of $\gtrsim 0.1$ – 1 rad above 10 Hz, which could be detectable with current GW detectors.

3. Gas effects may shift the GW frequency of non-GWC and GWC mergers formed during binary-single interactions, enhancing the prospects for detecting phase shifts by LIGO/Virgo/KAGRA. The influence of gas effects merits further elucidation through additional studies.
4. The phase shift from highly eccentric mergers could be significant, due to the enhancement of the frequency in the dominant GW mode, as also newly pointed out by Zwick et al. (2025a,e,d) and Takátsy et al. (2025).

Simulations were carried out on Cray XD2000 at the Center for Computational Astrophysics, National Astronomical Observatory of Japan. J.S. and K.H. are supported by the Villum Fonden grant No. 29466, and by the ERC Starting Grant no. 101043143 – BlackHoleMergs. L.Z. is supported by the European Union’s Horizon 2024 research and innovation program under the Marie Skłodowska-Curie grant agreement No. 101208914. J.T. is supported by the Alexander von Humboldt Foundation under the project no. 1240213 - HFST-P. The Center of Gravity is a Center of Excellence funded by the Danish National Research Foundation under grant No. 184.

APPENDIX

REFERENCES

- Abbott, R., Abbott, T. D., Abraham, S., et al. 2020, *PhRvL*, 125, 101102, doi: [10.1103/PhysRevLett.125.101102](https://doi.org/10.1103/PhysRevLett.125.101102)
- Acernese, F., Agathos, M., Agatsuma, K., et al. 2015, *Classical and Quantum Gravity*, 32, 024001, doi: [10.1088/0264-9381/32/2/024001](https://doi.org/10.1088/0264-9381/32/2/024001)
- Akutsu, T., Ando, M., Arai, K., et al. 2021, *Progress of Theoretical and Experimental Physics*, 2021, 05A101, doi: [10.1093/ptep/ptaa125](https://doi.org/10.1093/ptep/ptaa125)
- Antonini, F., Rodriguez, C. L., Petrovich, C., & Fischer, C. L. 2018, *MNRAS*, 480, L58, doi: [10.1093/mnras/sly126](https://doi.org/10.1093/mnras/sly126)
- Antonini, F., Toonen, S., & Hamers, A. S. 2017a, *ApJ*, 841, 77, doi: [10.3847/1538-4357/aa6f5e](https://doi.org/10.3847/1538-4357/aa6f5e)
- . 2017b, *ApJ*, 841, 77, doi: [10.3847/1538-4357/aa6f5e](https://doi.org/10.3847/1538-4357/aa6f5e)
- Arca Sedda, M., Berry, C. P. L., Jani, K., et al. 2020, *Classical and Quantum Gravity*, 37, 215011, doi: [10.1088/1361-6382/abb5c1](https://doi.org/10.1088/1361-6382/abb5c1)
- Banerjee, S. 2017, *MNRAS*, 467, 524, <http://adsabs.harvard.edu/abs/2017MNRAS.467..524B>
- Bartos, I., Kocsis, B., Haiman, Z., & Márka, S. 2017, *ApJ*, 835, 165, <http://adsabs.harvard.edu/abs/2017ApJ...835..165B>
- Belczynski, K., Daniel, E. H., Bulik, T., & O’Shaughnessy, R. 2016, *Nature*, 534, 512, <http://adsabs.harvard.edu/abs/2016Natur.534..512B>
- Bellovary, J. M., Mac Low, M. M., McKernan, B., & Ford, K. E. S. 2016, *ApJ*, 819, L17, <http://adsabs.harvard.edu/abs/2016ApJ...819L..17B>
- Chatzopoulos, E., & Wheeler, J. C. 2012, *ApJ*, 748, 42, doi: [10.1088/0004-637X/748/1/42](https://doi.org/10.1088/0004-637X/748/1/42)
- Chen, R., Chandramouli, R. S., Pozzoli, F., Busicchio, R., & Barausse, E. 2025a, arXiv e-prints, arXiv:2507.00694, doi: [10.48550/arXiv.2507.00694](https://doi.org/10.48550/arXiv.2507.00694)
- . 2025b, arXiv e-prints, arXiv:2507.00694, doi: [10.48550/arXiv.2507.00694](https://doi.org/10.48550/arXiv.2507.00694)

- Chen, Y.-X., Jiang, Y.-F., Goodman, J., & Ostriker, E. C. 2023, *ApJ*, 948, 120, doi: [10.3847/1538-4357/acc023](https://doi.org/10.3847/1538-4357/acc023)
- de Lluc Planas, M., Ramos-Buades, A., García-Quirós, C., et al. 2025, arXiv e-prints, arXiv:2504.15833, doi: [10.48550/arXiv.2504.15833](https://doi.org/10.48550/arXiv.2504.15833)
- DeLaurentiis, S., Epstein-Martin, M., & Haiman, Z. 2023, *MNRAS*, 523, 1126, doi: [10.1093/mnras/stad1412](https://doi.org/10.1093/mnras/stad1412)
- Delfavero, V., Ford, K. E. S., McKernan, B., et al. 2025, *ApJ*, 989, 67, doi: [10.3847/1538-4357/ade4c1](https://doi.org/10.3847/1538-4357/ade4c1)
- Dempsey, A. M., Li, H., Mishra, B., & Li, S. 2022, *ApJ*, 940, 155, doi: [10.3847/1538-4357/ac9d92](https://doi.org/10.3847/1538-4357/ac9d92)
- Dittmann, A. J., Dempsey, A. M., & Li, H. 2024, *ApJ*, 964, 61, doi: [10.3847/1538-4357/ad23ce](https://doi.org/10.3847/1538-4357/ad23ce)
- . 2025, arXiv e-prints, arXiv:2505.05555, doi: [10.48550/arXiv.2505.05555](https://doi.org/10.48550/arXiv.2505.05555)
- Dodici, M., & Tremaine, S. 2024, *ApJ*, 972, 193, doi: [10.3847/1538-4357/ad5cf2](https://doi.org/10.3847/1538-4357/ad5cf2)
- Dominik, M., Belczynski, K., Fryer, C., et al. 2012, *ApJ*, 759, 52, <http://adsabs.harvard.edu/abs/2012ApJ...759...52D>
- Duffell, P. C., Haiman, Z., MacFadyen, A. I., D’Orazio, D. J., & Farris, B. D. 2014, *ApJL*, 792, L10, <http://adsabs.harvard.edu/abs/2014ApJ...792L..10D>
- Dutta Roy, P., Mahapatra, P., Samajdar, A., & Arun, K. G. 2025, arXiv e-prints, arXiv:2503.11721, doi: [10.48550/arXiv.2503.11721](https://doi.org/10.48550/arXiv.2503.11721)
- Epstein-Martin, M., Tagawa, H., Haiman, Z., & Perna, R. 2025, *MNRAS*, 537, 3396, doi: [10.1093/mnras/staf237](https://doi.org/10.1093/mnras/staf237)
- Fabj, G., & Samsing, J. 2024, *MNRAS*, 535, 3630, doi: [10.1093/mnras/stae2499](https://doi.org/10.1093/mnras/stae2499)
- Fabj, G., Tiede, C., Rowan, C., Pessah, M., & Samsing, J. 2025, arXiv e-prints, arXiv:2510.07952, doi: [10.48550/arXiv.2510.07952](https://doi.org/10.48550/arXiv.2510.07952)
- Fragione, G., & Kocsis, B. 2019, *MNRAS*, 486, 4781, doi: [10.1093/mnras/stz1175](https://doi.org/10.1093/mnras/stz1175)
- Gamba, R., Breschi, M., Carullo, G., et al. 2023, *Nat. Astron.*, 7, 11, doi: [10.1038/s41550-022-01813-w](https://doi.org/10.1038/s41550-022-01813-w)
- Gayathri, V., Yang, Y., Tagawa, H., Haiman, Z., & Bartos, I. 2021, arXiv e-prints, arXiv:2104.10253, <https://arxiv.org/abs/2104.10253>
- Gayathri, V., Healy, J., Lange, J., et al. 2020, <https://arxiv.org/abs/2009.05461>
- Generozov, A., & Perets, H. B. 2022, arXiv e-prints, arXiv:2212.11301, doi: [10.48550/arXiv.2212.11301](https://doi.org/10.48550/arXiv.2212.11301)
- Gilbaum, S., Grishin, E., Stone, N. C., & Mandel, I. 2025, *ApJL*, 982, L13, doi: [10.3847/2041-8213/adb7dc](https://doi.org/10.3847/2041-8213/adb7dc)
- Goldreich, P., Lithwick, Y., & Sari, R. 2002, *Nature*, 420, 643, <http://adsabs.harvard.edu/abs/2002Natur.420..643G>
- Goodman, J. 2003, *MNRAS*, 339, 937, <http://adsabs.harvard.edu/abs/2003MNRAS.339..937G>
- Grishin, E., Gilbaum, S., & Stone, N. C. 2024, *MNRAS*, 530, 2114, doi: [10.1093/mnras/stae828](https://doi.org/10.1093/mnras/stae828)
- Gupte, N., Ramos-Buades, A., Buonanno, A., et al. 2024, <https://arxiv.org/abs/2404.14286>
- Hamers, A. S. 2021, *Research Notes of the American Astronomical Society*, 5, 275, doi: [10.3847/2515-5172/ac3d98](https://doi.org/10.3847/2515-5172/ac3d98)
- Hendriks, K., Zwick, L., & Samsing, J. 2024a, arXiv e-prints, arXiv:2408.04603, doi: [10.48550/arXiv.2408.04603](https://doi.org/10.48550/arXiv.2408.04603)
- Hendriks, K., Atallah, D., Martinez, M., et al. 2024b, arXiv e-prints, arXiv:2411.08572, doi: [10.48550/arXiv.2411.08572](https://doi.org/10.48550/arXiv.2411.08572)
- Inayoshi, K., Tamanini, N., Caprini, C., & Haiman, Z. 2017, *PhRvD*, 96, 063014, doi: [10.1103/PhysRevD.96.063014](https://doi.org/10.1103/PhysRevD.96.063014)
- Jiménez, M. A., & Masset, F. S. 2017, *MNRAS*, 471, 4917, doi: [10.1093/mnras/stx1946](https://doi.org/10.1093/mnras/stx1946)
- Kanagawa, K. D., Muto, T., Tanaka, H., et al. 2015, *ApJL*, 806, L15, <http://adsabs.harvard.edu/abs/2015ApJ...806L..15K>
- Kanagawa, K. D., Tanaka, H., & Szuszkiewicz, E. 2018, *ApJ*, 861, 140, <http://adsabs.harvard.edu/abs/2018ApJ...861..140K>
- Kinugawa, T., Inayoshi, K., Hotokezaka, K., Nakauchi, D., & T., N. 2014, *MNRAS*, 442, 2963, <http://adsabs.harvard.edu/abs/2014MNRAS.442.2963K>
- Kremer, K., Ye, C. S., Rui, N. Z., et al. 2020, *Astrophys. J. Supp. S.*, 247, 48, doi: [10.3847/1538-4365/ab7919](https://doi.org/10.3847/1538-4365/ab7919)
- Kumamoto, J., Fujii, M. S., & Tanikawa, A. 2018, arXiv e-prints, <https://arxiv.org/abs/1811.06726>
- Leigh, N. W. C., Geller, A. M., McKernan, B., et al. 2018, *MNRAS*, 474, 5672, doi: [10.1093/mnras/stx3134](https://doi.org/10.1093/mnras/stx3134)
- Li, J., Dempsey, A. M., Li, H., Lai, D., & Li, S. 2023, *ApJL*, 944, L42, doi: [10.3847/2041-8213/acb934](https://doi.org/10.3847/2041-8213/acb934)
- Li, R., & Lai, D. 2022, *MNRAS*, 517, 1602, doi: [10.1093/mnras/stac2577](https://doi.org/10.1093/mnras/stac2577)
- . 2024, *MNRAS*, 529, 348, doi: [10.1093/mnras/stae504](https://doi.org/10.1093/mnras/stae504)
- Li, Y.-J., Wang, Y.-Z., Tang, S.-P., & Fan, Y.-Z. 2025, arXiv e-prints, arXiv:2509.23897, doi: [10.48550/arXiv.2509.23897](https://doi.org/10.48550/arXiv.2509.23897)
- LIGO Scientific Collaboration, Aasi, J., Abbott, B. P., et al. 2015, *Classical and Quantum Gravity*, 32, 074001, doi: [10.1088/0264-9381/32/7/074001](https://doi.org/10.1088/0264-9381/32/7/074001)
- Liu, B., & Lai, D. 2018, *ApJ*, 863, 68, doi: [10.3847/1538-4357/aad09f](https://doi.org/10.3847/1538-4357/aad09f)
- Lousto, C. O., Zlochower, Y., Dotti, M., & Volonteri, M. 2012, *PhRvD*, 85, 084015, doi: [10.1103/PhysRevD.85.084015](https://doi.org/10.1103/PhysRevD.85.084015)

- McKernan, B., Ford, K. E. S., Bellovary, J., et al. 2018, *ApJ*, 866, 66, doi: [10.3847/1538-4357/aadae5](https://doi.org/10.3847/1538-4357/aadae5)
- Meiron, Y., Kocsis, B., & Loeb, A. 2017, *ApJ*, 834, 200. <http://adsabs.harvard.edu/abs/2017ApJ...834..200M>
- Morras, G., Pratten, G., & Schmidt, P. 2025, arXiv e-prints, arXiv:2503.15393, doi: [10.48550/arXiv.2503.15393](https://doi.org/10.48550/arXiv.2503.15393)
- Mueller, G., Baker, J., Barke, S., et al. 2019, in *Bulletin of the American Astronomical Society*, Vol. 51, 243, doi: [10.48550/arXiv.1907.11305](https://doi.org/10.48550/arXiv.1907.11305)
- O’Leary, R. M., Kocsis, B., & Loeb, A. 2009, *MNRAS*, 395, 2127, doi: [10.1111/j.1365-2966.2009.14653.x](https://doi.org/10.1111/j.1365-2966.2009.14653.x)
- O’Leary, R. M., Meiron, Y., & Kocsis, B. 2016, *ApJL*, 824, L12, doi: [10.3847/2041-8205/824/1/L12](https://doi.org/10.3847/2041-8205/824/1/L12)
- Ostriker, E. C. 1999, *ApJ*, 513, 252. <http://adsabs.harvard.edu/abs/1999ApJ...513..252O>
- Peters, P. C. 1964, *Physical Review*, 136, 1224, doi: [10.1103/PhysRev.136.B1224](https://doi.org/10.1103/PhysRev.136.B1224)
- Portegies Zwart, S. F., & McMillan, S. L. W. 2000, *ApJ*, 528, L17. <http://adsabs.harvard.edu/abs/2000ApJ...528L..17P>
- Qian, K., Li, J., & Lai, D. 2024, *ApJ*, 962, 143, doi: [10.3847/1538-4357/ad1b53](https://doi.org/10.3847/1538-4357/ad1b53)
- Quinlan, G. D., & Shapiro, S. L. 1989, *ApJ*, 343, 725, doi: [10.1086/167745](https://doi.org/10.1086/167745)
- Rastello, S., Amaro-Seoane, P., Arca-Sedda, M., et al. 2018, arXiv e-prints. <https://arxiv.org/abs/1811.10628>
- Rodriguez, C. L., & Antonini, F. 2018, *Astrophys. J.*, 863, 7, doi: [10.3847/1538-4357/aaea4](https://doi.org/10.3847/1538-4357/aaea4)
- Rodriguez, C. L., Chatterjee, S., & Rasio, F. A. 2016, *Phys. Rev. D.*, 93, 084029. <http://adsabs.harvard.edu/abs/2016PhRvD..93h4029R>
- Romero-Shaw, I., Lasky, P. D., & Thrane, E. 2022, *Astrophys. J.*, 940, 171, doi: [10.3847/1538-4357/ac9798](https://doi.org/10.3847/1538-4357/ac9798)
- Romero-Shaw, I., Lasky, P. D., Thrane, E., & Calderón Bustillo, J. 2020, *Astrophys. J. Lett.*, 903, L5, doi: [10.3847/2041-8213/abbe26](https://doi.org/10.3847/2041-8213/abbe26)
- Romero-Shaw, I., Stegmann, J., Tagawa, H., et al. 2025, arXiv e-prints, arXiv:2506.17105, doi: [10.48550/arXiv.2506.17105](https://doi.org/10.48550/arXiv.2506.17105)
- Romero-Shaw, I. M., Gerosa, D., & Loutrel, N. 2023, *Mon. Not. R. Astron. Soc.*, 519, 5352, doi: [10.1093/mnras/stad031](https://doi.org/10.1093/mnras/stad031)
- Rowan, C., Boehholt, T., Kocsis, B., & Haiman, Z. 2023, *MNRAS*, 524, 2770, doi: [10.1093/mnras/stad1926](https://doi.org/10.1093/mnras/stad1926)
- Rowan, C., Whitehead, H., Boehholt, T., Kocsis, B., & Haiman, Z. 2024a, *MNRAS*, 527, 10448, doi: [10.1093/mnras/stad3641](https://doi.org/10.1093/mnras/stad3641)
- Rowan, C., Whitehead, H., Fabj, G., et al. 2025a, *MNRAS*, 543, 132, doi: [10.1093/mnras/staf1449](https://doi.org/10.1093/mnras/staf1449)
- . 2025b, *MNRAS*, doi: [10.1093/mnras/staf547](https://doi.org/10.1093/mnras/staf547)
- Rowan, C., Whitehead, H., & Kocsis, B. 2024b, arXiv e-prints, arXiv:2412.12086, doi: [10.48550/arXiv.2412.12086](https://doi.org/10.48550/arXiv.2412.12086)
- Rozner, M., Generozov, A., & Perets, H. B. 2023, *MNRAS*, 521, 866, doi: [10.1093/mnras/stad603](https://doi.org/10.1093/mnras/stad603)
- Sagynbayeva, S., Li, R., Kuznetsova, A., et al. 2025, *ApJ*, 987, 216, doi: [10.3847/1538-4357/add934](https://doi.org/10.3847/1538-4357/add934)
- Samsing, J. 2018a, *PhRvD*, 97, 103014, doi: [10.1103/PhysRevD.97.103014](https://doi.org/10.1103/PhysRevD.97.103014)
- . 2018b, *Phys. Rev. D.*, 97, 103014. <http://adsabs.harvard.edu/abs/2018PhRvD..97j3014S>
- Samsing, J., Askar, A., & Giersz, M. 2018, *ApJ*, 855, 124. <http://adsabs.harvard.edu/abs/2018ApJ...855..124S>
- Samsing, J., & D’Orazio, D. J. 2018, *MNRAS*, 481, 5445, doi: [10.1093/mnras/sty2334](https://doi.org/10.1093/mnras/sty2334)
- Samsing, J., D’Orazio, D. J., Kremer, K., Rodriguez, C. L., & Askar, A. 2020a, *PhRvD*, 101, 123010, doi: [10.1103/PhysRevD.101.123010](https://doi.org/10.1103/PhysRevD.101.123010)
- Samsing, J., Hendriks, K., Zwick, L., D’Orazio, D. J., & Liu, B. 2025, *ApJ*, 990, 211, doi: [10.3847/1538-4357/ad9f3d](https://doi.org/10.3847/1538-4357/ad9f3d)
- Samsing, J., & Hotokezaka, K. 2021, *ApJ*, 923, 126, doi: [10.3847/1538-4357/ac2b27](https://doi.org/10.3847/1538-4357/ac2b27)
- Samsing, J., MacLeod, M., & Ramirez-Ruiz, E. 2014, *ApJ*, 784, 71, doi: [10.1088/0004-637X/784/1/71](https://doi.org/10.1088/0004-637X/784/1/71)
- Samsing, J., & Ramirez-Ruiz, E. 2017, *ApJL*, 840, L14, doi: [10.3847/2041-8213/aa6f0b](https://doi.org/10.3847/2041-8213/aa6f0b)
- Samsing, J., Bartos, I., D’Orazio, D. J., et al. 2020b, arXiv e-prints, arXiv:2010.09765. <https://arxiv.org/abs/2010.09765>
- . 2022, *Nature*, 603, 237, doi: [10.1038/s41586-021-04333-1](https://doi.org/10.1038/s41586-021-04333-1)
- Silber, K., & Tremaine, S. 2017, *ApJ*, 836, 39. <http://adsabs.harvard.edu/abs/2017ApJ...836...39S>
- Spera, M., Mapelli, M., Giacobbo, N., et al. 2019, *MNRAS*, 485, 889, doi: [10.1093/mnras/stz359](https://doi.org/10.1093/mnras/stz359)
- Stone, N. C., Metzger, B. D., & Haiman, Z. 2017, *MNRAS*, 464, 946. <http://adsabs.harvard.edu/abs/2017MNRAS.464..946S>
- Syer, D., Clarke, C. J., & Rees, M. J. 1991, *MNRAS*, 250, 505, doi: [10.1093/mnras/250.3.505](https://doi.org/10.1093/mnras/250.3.505)
- Szolgyen, A., & Kocsis, B. 2018, *Phys. Rev. Lett.*, 121, 101101. <http://adsabs.harvard.edu/abs/2018PhRvL.121j1101S>
- Tagawa, H., Haiman, Z., Bartos, I., & Kocsis, B. 2020a, *ApJ*, 899, 26, doi: [10.3847/1538-4357/aba2cc](https://doi.org/10.3847/1538-4357/aba2cc)
- Tagawa, H., Haiman, Z., & Kocsis, B. 2020b, *ApJ*, 898, 25, doi: [10.3847/1538-4357/ab9b8c](https://doi.org/10.3847/1538-4357/ab9b8c)
- Tagawa, H., Kimura, S. S., Haiman, Z., et al. 2022, *ApJ*, 927, 41, doi: [10.3847/1538-4357/ac45f8](https://doi.org/10.3847/1538-4357/ac45f8)

- Tagawa, H., Kocsis, B., Haiman, Z., et al. 2021a, *ApJL*, 907, L20, doi: [10.3847/2041-8213/abd4d3](https://doi.org/10.3847/2041-8213/abd4d3)
- . 2021b, *ApJ*, 908, 194, doi: [10.3847/1538-4357/abd555](https://doi.org/10.3847/1538-4357/abd555)
- Takátsy, J., Zwick, L., Hendriks, K., et al. 2025, *Classical and Quantum Gravity*, 42, 215006, doi: [10.1088/1361-6382/ae0fd4](https://doi.org/10.1088/1361-6382/ae0fd4)
- Tanikawa, A., Yoshida, T., Kinugawa, T., et al. 2022, *ApJ*, 926, 83, doi: [10.3847/1538-4357/ac4247](https://doi.org/10.3847/1538-4357/ac4247)
- The LIGO Scientific Collaboration, The Virgo Collaboration, & the KAGRA Collaboration. 2025a, arXiv e-prints, arXiv:2508.18082, doi: [10.48550/arXiv.2508.18082](https://doi.org/10.48550/arXiv.2508.18082)
- The LIGO Scientific Collaboration, the Virgo Collaboration, & the KAGRA Collaboration. 2025b, arXiv e-prints, arXiv:2508.18083, doi: [10.48550/arXiv.2508.18083](https://doi.org/10.48550/arXiv.2508.18083)
- Thompson, T. A., Quataert, E., & Murray, N. 2005, *ApJ*, 630, 167, <http://adsabs.harvard.edu/abs/2005ApJ...630..167T>
- Trani, A. A., Quaini, S., & Colpi, M. 2024, *A&A*, 683, A135, doi: [10.1051/0004-6361/202347920](https://doi.org/10.1051/0004-6361/202347920)
- Vaccaro, M. P., Mapelli, M., Périgois, C., et al. 2024, *A&A*, 685, A51, doi: [10.1051/0004-6361/202348509](https://doi.org/10.1051/0004-6361/202348509)
- Vijaykumar, A., Tiwari, A., Kapadia, S. J., Arun, K. G., & Ajith, P. 2023, *ApJ*, 954, 105, doi: [10.3847/1538-4357/acd77d](https://doi.org/10.3847/1538-4357/acd77d)
- Wang, M., Ma, Y., Li, H., et al. 2025a, *ApJ*, 983, 114, doi: [10.3847/1538-4357/adbf8e](https://doi.org/10.3847/1538-4357/adbf8e)
- Wang, M., Wu, Q., & Ma, Y. 2025b, arXiv e-prints, arXiv:2507.07715, doi: [10.48550/arXiv.2507.07715](https://doi.org/10.48550/arXiv.2507.07715)
- Wang, Y., Zhu, Z., & Lin, D. N. C. 2024, *MNRAS*, 528, 4958, doi: [10.1093/mnras/stae321](https://doi.org/10.1093/mnras/stae321)
- Wen, L. 2003, *ApJ*, 598, 419, doi: [10.1086/378794](https://doi.org/10.1086/378794)
- Whitehead, H., Rowan, C., Boekholt, T., & Kocsis, B. 2024, *MNRAS*, 531, 4656, doi: [10.1093/mnras/stae1430](https://doi.org/10.1093/mnras/stae1430)
- Whitehead, H., Rowan, C., & Kocsis, B. 2025a, *MNRAS*, 543, 3768, doi: [10.1093/mnras/staf1686](https://doi.org/10.1093/mnras/staf1686)
- . 2025b, *MNRAS*, 542, 1033, doi: [10.1093/mnras/staf1271](https://doi.org/10.1093/mnras/staf1271)
- Wong, K. W. K., Baibhav, V., & Berti, E. 2019, *MNRAS*, 488, 5665, doi: [10.1093/mnras/stz2077](https://doi.org/10.1093/mnras/stz2077)
- Xue, L., Tagawa, H., Haiman, Z., & Bartos, I. 2025, arXiv e-prints, arXiv:2504.19570, doi: [10.48550/arXiv.2504.19570](https://doi.org/10.48550/arXiv.2504.19570)
- Yagi, K., & Seto, N. 2011, *PhRvD*, 83, 044011, doi: [10.1103/PhysRevD.83.044011](https://doi.org/10.1103/PhysRevD.83.044011)
- Yang, S.-C., Han, W.-B., Tagawa, H., Li, S., & Zhang, C. 2025, *ApJL*, 988, L41, doi: [10.3847/2041-8213/adeaad](https://doi.org/10.3847/2041-8213/adeaad)
- Yang, Y., Bartos, I., Gayathri, V., et al. 2019a, *PhRvL*, 123, 181101, doi: [10.1103/PhysRevLett.123.181101](https://doi.org/10.1103/PhysRevLett.123.181101)
- . 2019b, arXiv e-prints, arXiv:1906.09281, <https://arxiv.org/abs/1906.09281>
- Zevin, M., Romero-Shaw, I. M., Kremer, K., Thrane, E., & Lasky, P. D. 2021, *Astrophys. J. Lett.*, 921, L43, doi: [10.3847/2041-8213/ac32dc](https://doi.org/10.3847/2041-8213/ac32dc)
- Zwick, L., Hendriks, K., Saini, P., et al. 2025a, arXiv e-prints, arXiv:2511.04540, doi: [10.48550/arXiv.2511.04540](https://doi.org/10.48550/arXiv.2511.04540)
- Zwick, L., Takátsy, J., Saini, P., et al. 2025b, arXiv e-prints, arXiv:2503.24084, doi: [10.48550/arXiv.2503.24084](https://doi.org/10.48550/arXiv.2503.24084)
- . 2025c, arXiv e-prints, arXiv:2503.24084, doi: [10.48550/arXiv.2503.24084](https://doi.org/10.48550/arXiv.2503.24084)
- . 2025d, *ApJ*, 991, 131, doi: [10.3847/1538-4357/adf6b8](https://doi.org/10.3847/1538-4357/adf6b8)
- Zwick, L., Tiede, C., Trani, A. A., et al. 2024, *PhRvD*, 110, 103005, doi: [10.1103/PhysRevD.110.103005](https://doi.org/10.1103/PhysRevD.110.103005)
- Zwick, L., Hendriks, K., O'Neill, D., et al. 2025e, *PhRvD*, 112, 063005, doi: [10.1103/lz7k-bvjf](https://doi.org/10.1103/lz7k-bvjf)